

# Transient Period of the Acceleration-Produced Burning Rate Augmentation

Takashi Niioka,\* Tohru Mitani,† and Shinichi Ishii‡  
*National Aerospace Laboratory, Kakuda Branch, Miyagi, Japan*

This paper presents an experimental study on the transient burning rate augmentation of a 9.0% aluminized composite propellant in centrifugal acceleration fields. The centrifuge used was comprised of a combustion bomb, a ballast tank, and four nitrogen tanks mounted on a 1100° turn-table. The burning rate variation was obtained from the variation of the flame image heights on the dry-plate, which were recorded periodically by a continuous recording camera. The experiments were conducted within a range of acceleration from 0 to 60 g, with pressures between 20-40 kg/cm<sup>2</sup>. The results indicate that the burning rate increases from the basic (zero g), burning rate, reaches a maximum at 1-15 sec after ignition, and its value is 1.3-1.4 times as large as the basic value within this experimental range.

## Introduction

IT has been reported that the performance of solid rocket motors is dependent upon the spin rate of the motor, and this so-called spin effect is due to spin induced changes in combustion phenomena. The fundamental theory of Crowe and Willoughby<sup>1</sup> indicates that aluminum particles contained in the propellant are retained on the combustion surface, and become a heat source responsible for an increased burning rate. Based on this study, the average burning rate augmentation of a variety of propellants has been obtained by many investigators during the past ten years by means of strand burners,<sup>2</sup> slab motors,<sup>3,4</sup> and spinning motor methods.<sup>5</sup> Various analytical models<sup>6,7</sup> of the phenomenon have also been developed, and attempts made toward their application.

Most of the investigators, however, have treated this problem as a steady phenomenon in the mean since it is rather complicated. In actual performance, for instance, the burning rate augmentation produced by acceleration ought to change in proportion to the burning time. This transient acceleration sensitivity of solid propellants is a problem one should not ignore in the design of spin-stabilized vehicles. For several years the authors have been researching the effects of the acceleration environment on the combustion mechanism of various solid propellants. We were prompted by the paucity of reports on the continuous measurement of the burning rate in the acceleration field to develop and concentrate especially on the problem of the transient period. A few studies have been made to investigate this subject. These results indicate that the burning rate increases from the basic burning rate to a maximum; after that it decreases toward a steady value in proportion to burning time as shown in Fig. 1. The data of the burning rate variation with time, obtained by Northam,<sup>8</sup> was calculated from the pressure histories of a slab motor. Cowles and Netzer<sup>9</sup> presented the effect of the strand length on augmentation, but the consecutive measurement of the transient burning rate during burning has never been reported until this present study. In addition from an analytical standpoint there are many problems remaining unsolved con-

cerning the solid propellant combustion mechanisms in the acceleration field. The experiment presented in this paper was conducted in order to confirm the transient behavior calculated by Northam, and to study in detail the effect of the pressure and the acceleration force on the transient burning rate by means of a strand burner mounted on a turn-table.

## Experimental Equipments and Procedures

The centrifuge used, which is similar to that used by Willoughby et al.<sup>7</sup> was comprised of a combustion bomb, a ballast tank, and 4 nitrogen tanks mounted on a 1100° turn-table producing up to 500 rpm as shown in Fig. 2. This turn-table was driven at constant rpm by an induction motor with a coupling device during a given test. The combustion bomb (1) the number in parenthesis shows each equipment in Fig. 2) was pressurized to a predetermined level. Just before ignition the solenoid valve (5) was opened and nitrogen gas, which prevents accumulation of smoke in the optical path, flowed into the bomb from four nitrogen tanks (6-9). Simultaneously the bomb pressure was adjusted by exhausting the gas from the valve (19), and controlled remotely by the valve (11), and then ignited. The combustion gas and the nitrogen gas flow (indicated by arrows in Fig. 2) are discharged from the center of the turn-table after the gases are purified by the filter (12). The greater amount of gases were discharged from the valve (19), and fine pressure adjustment was made by means of the hand-operated valve (11) connected by flexible tubing (17) to the rotary joint (21), which was mounted in the center of the turn-table.

The main part of the apparatus is shown in Fig. 3. A propellant sample of 17×8.5 mm<sup>2</sup> combustion surface area and 75 mm length was set on the platform at the center of the bomb. A nitrogen flow past the strand sample at almost the same velocity as the combustion gas flow velocity prevented the accumulation of smoke in the optical path. The acceleration vector was always normal to and directed into the combustion surface. The propellant used was a composite propellant (CTPB-AP) containing an aluminum powder concentration of 9.0%. The burning rate variation was obtained from the variation of the flame heights (Fig. 4) on the dry-plate recorded periodically through a slit by a continuous recording camera, which was fixed on the side of the turn-table. The mean burning rate of the small time interval between two images was obtained. Therefore the mean burning rate of the larger time interval can be determined in proportion to the decreased revolution of the turn-table, and each datum at minimum acceleration 15 g is the mean during a time

Presented as Paper 75-1331 at the AIAA/SAE 11th Propulsion Conference, Anaheim, Calif., Sept. 29-Oct. 1, 1975; submitted Oct. 3, 1975; revision received Feb. 24, 1976. The authors would like to thank M. Izumikawa and M. Takahashi for their technical assistance.

Index category: Combustion in Heterogeneous Media; Fuels and Propellants, Properties of.

\*Principal Research Officer.

†Research Officer.

‡Chief, Solid Propellant Rocket Section.

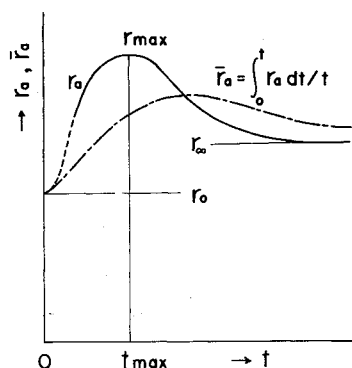


Fig. 1 Schematic diagram of the burning rate variation with time.

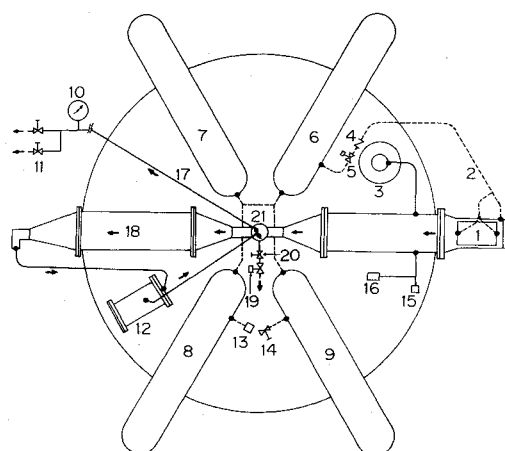


Fig. 2 Experimental apparatus: (1) combustion chamber, (2) nitrogen pipe, (3) rupture disc, (4) check valve, (5) solenoid valve, (6)-(9) nitrogen tank, (10) pressure gauge, (11) control valve, (12) filter, (13) pressure transducer (nitrogen tank), (14) nitrogen port, (15) pressure transducer (combustion chamber), (16) pressure transducer (used for control), (17) flexible tube, (18) counter balance, (19) solenoid valve, (20) exhaust valve, (21) rotary joint.

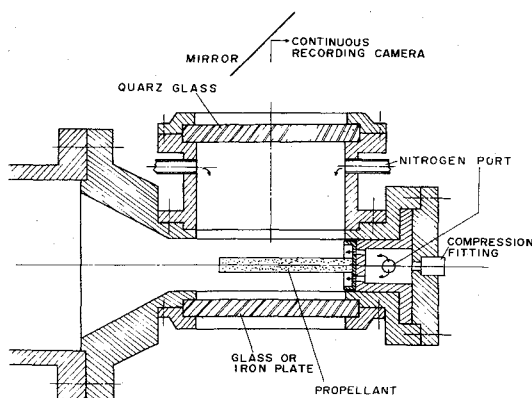


Fig. 3 Strand burner and optical equipment.

interval of about 0.4 sec. The experiments were conducted within the range of accelerations 0 g, 15-60 g with pressures 20-40 kg/cm<sup>2</sup>.

The accuracy of each test depends on the reading technique of images recorded on the film. But the largest error is induced by the low reproducibility particular to the experiments in the acceleration field. Therefore, the results should be understood in terms of probability by many firing tests.

## Results

Figures 5-7 show experimental results of burning rate change with time for the propellant described in the

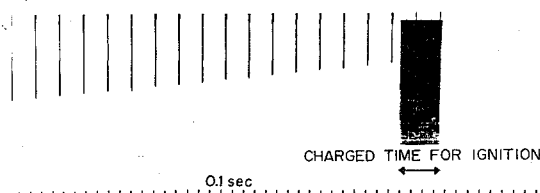


Fig. 4 Flame images taken through a slit.

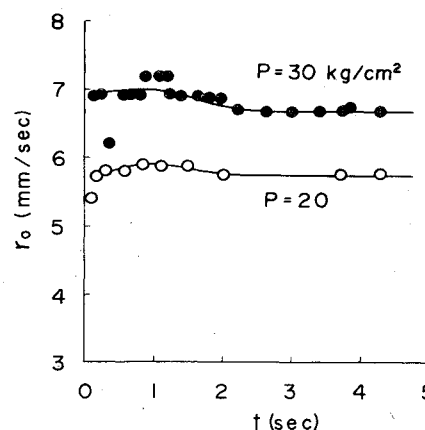


Fig. 5 The variation of the burning rate in the acceleration of zero g.

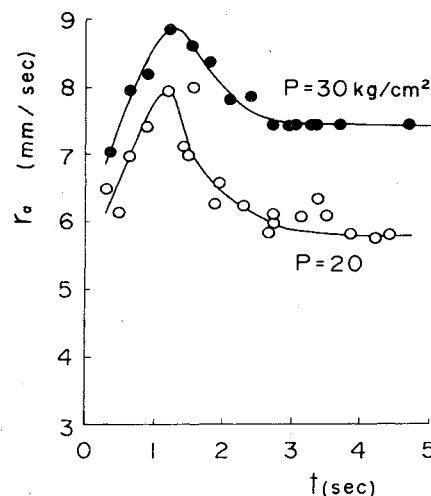


Fig. 6 The variation of the burning rate in the acceleration of 30 g.

preceding section. Combustion bomb pressure, either  $P=20$  or  $30 \text{ kg/cm}^2$ , is the parameter. Although the extinction test of the burning strand confirmed that the combustion surface regressed uniformly even after several seconds, the boundary-line of the images was not always distinct because of a slight accumulation of smoke, especially immediately after ignition. Accordingly the data in Figs. 5-7 was obtained from several initial experiments. Curves have been drawn to indicate the apparent trend of the data.

The results indicate that the burning rate ( $r$ ) increases from the basic (zero g) burning rate ( $r_0$ ), and reaches a maximum ( $r_{\max}$ ) at 1-1.5 sec after ignition, and its value is 1.3-1.4 times as large as the basic value within this experimental range. After that the burning rate decreases toward a steady value ( $r_{\infty}$ ) higher than the basic value at 2-3 sec after ignition. The burning rate at ignition seemed to have a tendency to take the smaller value as its basic rate. In general the time average burning rate ( $r_a$ ) as shown in Fig. 1, was obtained by assuming that the burning rate at ignition was equal to  $r_0$ , was larger than those of a slab motor during the same burning time. The transient characteristic was recorded even in a lower

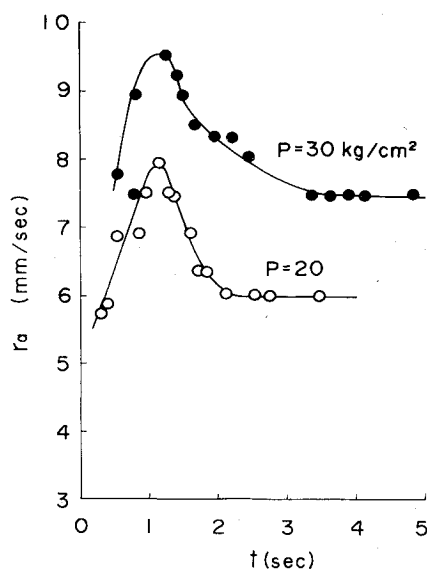


Fig. 7 The variation of the burning rate in the acceleration of 45 g.

acceleration field than the critical acceleration<sup>10</sup> of the slab motor experiment.

The acceleration and pressure dependence of  $r_{\max}$ ,  $r_{\infty}$ , and  $t_{\max}$  are shown in Figs. 8 and 9, respectively. The scatterings of the data are also indicated in these figures. Since these figures indicate the aspects of the main positions in Figs. 5-7, these arrangements are useful for expressing Fig. 5-7 by mathematics,<sup>‡</sup> and calculating the predicted time-pressure curve of an arbitrary spin-stabilized motor. Although the time ( $t_{\max}$ ) takes a maximum value which is small compared with the results calculated from the time-pressure trace of the slab motor by Northam<sup>8</sup>. This is perhaps due to the difference of the mass median diameter of aluminum powder, i.e. the particle size used by Northam is  $7\mu$ , and the authors' is  $48\mu$ . Moreover, considering the value of  $t_{\max}$  is not affected very much by the pressure, although its time in Northam's study was affected, it is assumed that the aluminum powder size influences the combustion characteristics considerably. It is not yet conclusive that the differences between the Northam's data and this experiment are caused by the difference in experimental technique besides the aluminum powder. But more detailed experiments with larger combustion surface area are required because of the pitting phenomenon on accelerated combustion surfaces. In addition, it was found that the value of  $t_{\max}$  decreased as the acceleration increased, and that the value of  $r_{\max}/r_0$  decreased, and the value of  $r_{\infty}/r_0$  increased as the pressure increased.

<sup>‡</sup>The example of the mathematical expression for the curves in Figs. 5-7 is as follows.

$$\frac{r_a - r_0}{r_{\max} - r_0} = \left\{ \frac{t}{t_{\max}} \exp\left(1 - \frac{t}{t_{\max}}\right) \right\}^n \quad \left(0 \leq \frac{t}{t_{\max}} < K\right)$$

$$\frac{r_a - r_0}{r_{\infty} - r_0} = (K - 1)K^{n-1} \left\{ \exp\left(1 - \frac{t}{t_{\max}}\right) \right\}^n \quad \left(K \leq \frac{t}{t_{\max}}\right)$$

where  $K$  is obtained from the equation

$$K^{n-1} \exp\left\{n(1-K)\right\} = \frac{r_{\infty} - r_0}{r_{\max} - r_0}$$

$n$  is chosen in order that these equations fit with the curves as much as possible, and each parameter in the equations must be expressed as a function of pressure and acceleration force.

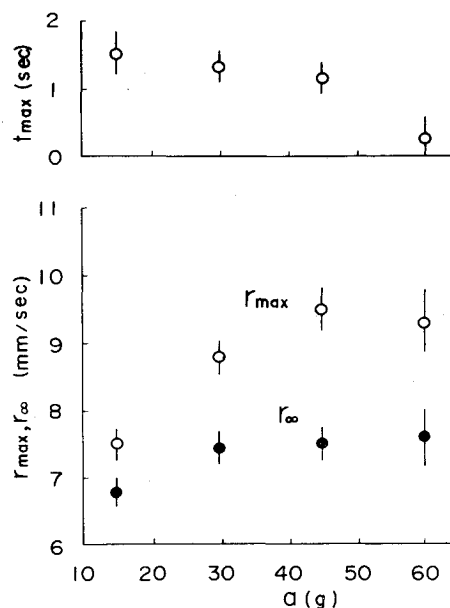


Fig. 8 The variation of  $r_{\max}$ ,  $r_{\infty}$ , and  $t_{\max}$  with acceleration. ( $P = 30 \text{ kg/cm}^2$ ,  $r_0 = 6.71 \text{ mm/sec}$ ).

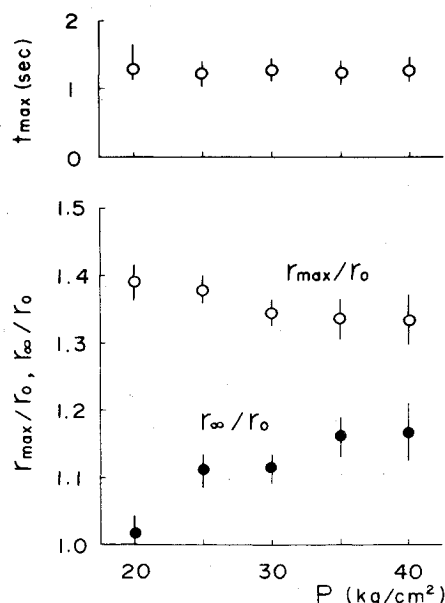


Fig. 9 The variation of  $r_{\max}$ ,  $r_{\infty}$ , and  $t_{\max}$  with pressure (acceleration = 30 g).

## Discussion

In general the variation of the time-average burning rate augmentation ( $\overline{r_a/r_0}$ ) with acceleration, which has been obtained by many investigators, has a tendency to approach a constant value. Since  $r_{\max}/r_0$  decreases, and  $r_{\infty}/r_0$  increases as the pressure increases as shown in Fig. 9, the time- $\overline{r_a/r_0}$  curve ought to show a small change. Accordingly in higher pressures the average burning rate augmentation ( $\overline{r_a/r_0}$ ) more easily approaches a constant value at low acceleration in composite propellants. This tendency is consistent with our results obtained with slab motor experiments.<sup>11</sup> Moreover the observation (shown in Fig. 9) that  $r_{\max}$  increases, and  $t_{\max}$  decreases in proportion to acceleration, agrees with those predicted by the experimental result based on a slab motor, or Crowe's model.

A clear explanation on the transient period seems to be lacking, although there are many possibilities of qualitative discussion we have already mentioned. We will now give an



Fig. 10 Web part of the extinguished combustion surface of 200° spinning motor.<sup>5</sup>

outline of an analytical model for solving the transient behavior. The quasi-steady models presented by Willoughby et al.<sup>7</sup> and Crowe<sup>12</sup> state that spherical metal-metal oxide globules retained in pits in the combustion surface (Fig. 10) deform into ellipsoids as burning continues and agglomeration proceeds, and then deform into irregularly shaped platelets which characterize the steady period. There probably is no serious change or addition in this estimation of the drag force and the heat feedback. The most important point, however, is the variation of the pit formation and the globule mass with the burning time.

On the assumption that the pit begins to develop at ignition as shown in Fig. 11, the pit diameter ( $D_p$ ) changes with time ( $t$ ) as follows:

$$D_p = 2r_0 \left\{ \frac{(r_a/r_0)_p - 1}{(r_a/r_0)_p + 1} \right\}^{1/2} \cdot t \quad (1)$$

where  $(r_a/r_0)_p$  indicated the ratio of the burning rate at pit to the basic value ( $r_0$ ), and equals  $(\cos\theta)^{-1}$ . It can be seen that the overall burning rate augmentation, which has been discussed above as the main subject of this study, is the weighted value of the portion covered by pits having a large augmentation.

$$\frac{r_a}{r_0} = \left\{ \left( \frac{r_a}{r_0} \right)_p - 1 \right\} \cdot \frac{\pi}{4} D_p^2 \cdot N_p + 1 \quad (2)$$

where  $N_p$  is the pit density or number of pits per unit area, and must be expressed by the number of retained aluminum particles on the accelerated combustion surface and their size (for example Eq. (10) in Ref 4). Although further investigation is necessary for  $N_p$ , any analytical model used to explain the transient period, must include the growing mechanism of pits on the combustion surface as previously mentioned.

In the transient period the mass of the aluminum and/or aluminum oxide globules in the pits are variable with time. The mass change is expressed by the subtraction of the combustion rate of the globule from the agglomeration rate. Since

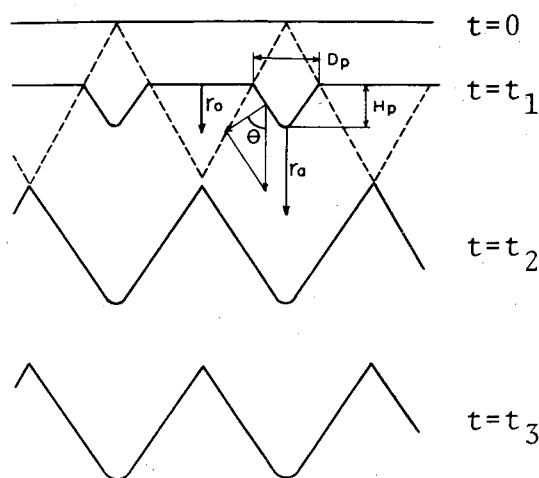


Fig. 11 The development of pits.

the combustion rate is in proportion to the globule diameter when the globule is considered to be a sphere

$$\frac{d}{dt} \left( \frac{\pi}{6} \rho_{al} D_{al}^3 \right) = r_a \rho_s w \cdot \frac{1}{N_p} \cdot G_a - K \cdot D_{al} \quad (3)$$

where  $\rho_{al}$  represents the aluminum density,  $\rho_s$  the propellant density,  $w$  the aluminum content,  $D_{al}$  the globule diameter,  $G_a$  the retained fraction of aluminum defined by Eq. (8) in Ref. 4 (which is determined by assuming a log-normal distribution of aluminum particle size, and the Stokes' law for the drag coefficient), and  $K$  the constant. A few problems remain unsolved in the agglomeration mechanism, and some corrections due to the globule shape are necessary for Eq. (3), but fundamentally Eq. (3) must be solved in order to clarify the transient period.

$(r_a/r_0)_p$  decreases as burning proceeds and agglomeration proceeds according to Eq. (3), because the drag force increases, and the globules gradually separate from the combustion surface due to globule deformation. This is confirmed experimentally by observing the pit shape.<sup>5</sup> Since  $D_p$ , on the other, increases in proportion to time, and takes a constant diameter determined by  $N_p$ , the transient behavior obtained experimentally is also theoretically predicted by Eq. (2). Solving the simultaneous equations for the balance of the drag and the acceleration force, the heat-feedback, the pit formation, and the globule growth will give the variation of the burning rate with time. Our primary assertion is that the most important aspect is proper conception of the overall burning rate.

## Conclusion

The results of the experiments conducted by means of the turn-table centrifuge with a range of acceleration up to 60 g, and pressure from 20 to 40 kg/cm<sup>2</sup>, show that the burning rate increases from the basic rate in proportion to the burning time. It reaches a maximum at 1-1.5 sec after ignition, and its value is 1.3-1.4 times as large as the basic value within this experimental range. The aspects of the transient burning rate curve with time approximately agree with those calculated by past studies of pressure histories of slab motor experiments, or predicted by theories developed previously. To clarify the transient behavior, however, the growing mechanism of pits on the combustion surface and the concept of the overall burning rate must be included in future analytical models.

## References

- 1 Crowe, C.T. and Willoughby, P.G., "Effect of Spin on the Internal Ballistics of a Solid Propellant Motor," AIAA Paper 66-523, Los Angeles, Calif., 1966.

<sup>2</sup>Sturm, E.J. and Reichenbach, R.E., "An Experimental Study of the Burning Rates of Aluminized Composite Solid Propellants in Acceleration Fields," AIAA Paper 68-529, Atlantic City, N.J., 1968.

<sup>3</sup>Northam, G.B., "Effects of Steady-State Acceleration on Combustion Characteristics of an Aluminized Composite Solid Propellant," NASA TN D-4914, 1968.

<sup>4</sup>Ishii, S., Niioka, T., and Mitani, T., "An Analytical and Experimental Study for Solid Propellant Combustion in an Acceleration Field," *Combustion Science and Technology*, Vol. 8, 1973, p. 177.

<sup>5</sup>Niioka, T., Mitani, T., and Ishii, S., "Observation of the Combustion Surface by Extinction Tests of Spinning Solid Propellant Rocket Motors," *Eleventh International Symposium on Space Technology and Science*, Tokyo, 1975.

<sup>6</sup>Glick, R.L., Hodge, B.K., and Caveny, L.H., "Effect of Acceleration of the Burning Rate of Composite Propellants," AIAA Paper 67-470, Washington, D.C., 1970.

<sup>7</sup>Willoughby, P.G., Crowe, C.T., and Baker, K.L., "A Photographic and Analytical Study of Composite Propellant Com-

bustion in an Acceleration Field," AIAA Paper 69-173, New York, N.Y., 1969.

<sup>8</sup>Northam, G.B., "Effects of the Acceleration Vector on Transient Burning Rate of an Aluminized Solid Propellant," *Journal of Spacecraft and Rockets*, Vol. 8, Nov. 1971, pp. 1133-1137.

<sup>9</sup>Cowles, D. and Netzer, D., "The Effect of Acceleration on Composite Propellant Combustion," *Combustion Science and Technology*, Vol. 3, 1971, p. 215.

<sup>10</sup>Niioka, T. and Mitani, T., "Independent Region of Acceleration in Solid Propellant Combustion," *AIAA Journal*, Vol. 12, Dec. 1974, pp. 1759-1761.

<sup>11</sup>Ishii, S., Niioka, T., and Mitani, T., "Combustion of Composite Propellants in Acceleration Field," National Aerospace Laboratory, TR-354, 1973, Miyagi, Japan (in Japanese).

<sup>12</sup>Crowe, C.T., "An Unified Model for the Acceleration-Produced Burning Rate Augmentation of Metalized Solid Propellants," *Combustion Science and Technology*, Vol. 5, 1972, p. 55.

## *From the AIAA Progress in Astronautics and Aeronautics Series . . .*

### **THERMAL CONTROL AND RADIATION—v. 31**

*Edited by C.-L. Tien, University of California, Berkeley*

Twenty-eight papers concern the most important advances in thermal control as related to spacecraft thermal design, and in radiation phenomena in the thermal environment of space, covering heat pipes, thermal control by other means, gaseous radiation, and surface radiation.

Heat pipe section examines characteristics of several wick materials, a self-priming pipe and development models, and the design and fabrication of a twelve-foot pipe for the Orbiting Astronomical Observatory C, and the 26-inch diode for the ATS-F Satellite.

Other thermal control methods examined include alloys, thermal control coatings, and plasma cleaning of such coatings. Papers examine the thermal contact resistance of bolted joints and electrical contacts, with role of surface roughness in thermal conductivity.

Gaseous radiation studies examine multidimensional heat transfer, thermal shielding by injection of absorbing gases into the boundary layer, and various gases as thermal absorbing media. Surface studies deal with real surface effects on roughened, real-time contaminated surfaces, and with new computational techniques to computer heat transfer for complex geometries, to enhance the capabilities and accuracy of radiation computing.

*523 pp., 6 x 9, illus. \$12.95 Mem. \$18.50 List*

TO ORDER WRITE: Publications Dept., AIAA, 1290 Avenue of the Americas, New York, N. Y. 10019